Journal of Physics: Conference Series

Magnetic Properties and Mössbauer spectroscopy of $NdFe_{1-x}Mn_xO_3$

To cite this article: J Lazurova *et al* 2015 *J. Phys.: Conf. Ser.* **592** 012117

Journal of Physics: Conference Series **592** (2015) 012117 doi:10.1088/1742-6596/592/1/012117

Magnetic Properties and Mössbauer spectroscopy of $NdFe_{1-x}Mn_xO_3$

J Lazurova[1], M Mihalik[1], M Mihalik jr.[1], M Vavra[1], M Zentkova[1], J Briancin[2], M Perovic[3], V Kusigerski[3], O Schneeweiss[4], P Roupcova[4], K V Kamenev[5], M Misek[5], Z Jaglicic[6]

[1]Institute of Experimental Physics, SAS, Watsonova 47, Kosice, Slovakia
[2]Institute of Geotechnics, SAS, Watsonova 45, Kosice, Slovakia
[3]The Vinca Institute, University of Belgrade, 11001 Belgrade, Serbia
[4]Institute of Physics of Materials, ASCR, v. v. i. Zizkova 22, Brno, Czech Republic
[5]CSEC and School of Engineering, University of Edinburgh, Edinburgh, UK
[6]IMPM & FGG, Jadranska 19, 1000 Ljubljana, Slovenia

E-mail: mihalik@saske.sk

Abstract The effect of particle reduction to nanoscale size and substitution of Mn^{3+} ions for Fe^{3+} ions on the crystal structure, lattice dynamics, Mössbauer spectra and magnetic properties in $NdFe_{1-x}Mn_xO_3$ compounds have been studied. X-ray powder diffraction and Raman spectroscopy revealed that the Jahn-Teller distortion of lattice dominates for samples with $x > 0.4$. The average particle size of $NdFeO_3$ nanoparticles (NAP) increases with annealing at 600°C from about 15 nm to 25 nm. The presence of superparamagnetic particles was indicated by Mössbauer measurements in $NdFeO_3$ NAP system. Sextets in $NdFe_{1-x}Mn_xO_3$ Mössbauer spectra can be modelled with several local environments of Fe^{3+} induced by substitution. The reduction of dimensionality and the substitution induce a decrease of the Néel temperature T_{N1} from 691 K to 544 K for NAP or to 356 K for $x = 0.4$, however the temperature of spin reorientation T_{SR} increases with substitution. The saturated magnetization obtained at 1.9 K increases and ferromagnetic component is removed below T_{SR} with the substitution.

1. Introduction

The physical and structural properties of $NdFeO_3$ are widely studied and they attract large attention due to interesting magnetic properties such as spin-reorientation phase transition [1]. Magnetic properties of $NdFeO_3$ are mostly determined by Fe-Fe, Fe-Nd and Nd-Nd exchange interactions. Magnetic ordering of Fe^{3+} ions creates a canted antiferromagnetic ordering of G-type below the Néel temperature at about $T_{N1} = 690$ K and the magnetic moments of Fe^{3+} exhibit spin reorientation from G_x type to combination of G_x and Gz type in the region from 100 K to 200 K. The moments of Nd were found to undergo a collective C-type antiferromagnetic ordering at $T_{N2} = 1.5$ K [2]. In our paper we study the effect of nano-metric size and substitution of the Mn^{3+} ion for the Fe^{3+} ion on the crystal structure, lattice dynamics, magnetic environment of iron and magnetization in $NdFe_{x-1}Mn_xO_3$ system.

2. Sample preparation and experimental details

$NdFeO_3$ nanoparticles (NAP) were prepared by the self-propagating high-temperature synthesis (SHS) which is based on a brief, exothermic burning reaction between oxidizing agent (potassium nitrate),

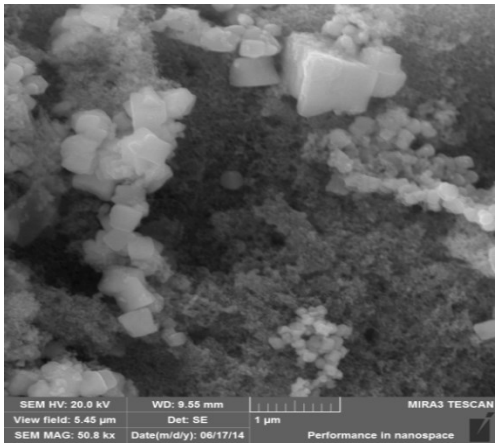

Figure 1. SEM image of $NdFeO_3$ nanoparticles annealed at 600°C/2h in air.

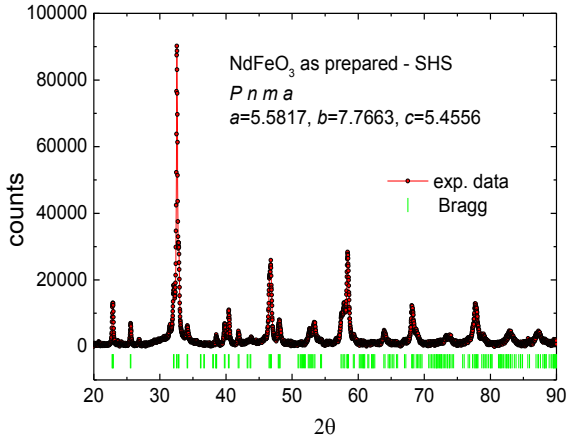

Figure 2. X-ray diffraction pattern of as prepared $NdFeO_3$ nanoparticles

organic fuel (glucose) and relevant metal nitrates [3]. The as prepared samples were annealed at 600°C for 2 hours in air using a muffle furnace. Ingots of $NdFe_{x-1}Mn_xO_3$ compounds have been grown by the optical floating technique (OFT) in a mirror furnace equipped with four mirrors. Stoichiometric ratio of starting materials Nd_2O_3, Fe_2O_3 and MnO_2 was mixed in the agate mortar in order to obtain homogenous powder. The powders were pressed into rods by isostatic cold pressing and sintered at 1100°C in air for 20 hours. The crystals were grown in air atmosphere with grown rate of 7 mm/hr and 15 rpm rotation of both shafts.

All samples have been characterized by scanning electron microscope (SEM) methods including the energy - dispersive X-ray (EDX) microanalysis on Mira III FE SEM produced by Tescan. Crystal structure of all samples was investigated by X-ray powder diffraction (XRD) technique on different diffractometers always in the Bragg-Brentano geometry. XRD on $NdFeO_3$ nanoparticles was studied by a D8 (Bruker) diffractometer using Cu $K_{\alpha1,\alpha2}$ doublet radiation. Crystal structure of $NdFe_{x-1}Mn_xO_3$ for $x \leq 0.4$ was determined by the X'Pert (PanAnalytical) diffractometer powered by Co $K_{\alpha1,\alpha2}$ doublet radiation with a help of qualitative analysis provided by HighScore® software and the JCPDS PDF-4 database. For a quantitative analysis HighScore plus® with Rietveld structural models based on the ICSD database was applied. Crystallographic data of samples with higher Mn content were taken from [4]. Raman experiment was performed on the Jobin-Yvon LabRAM spectrometer (Horiba Inc.). The spectrometer was equipped with He-Ne laser (λ = 632.8 nm) which was used for excitation, charge coupled device (CCD) detector and notch filter which filtered out the Raman shifts smaller than 85 cm^{-1}. The Raman spectra were collected with 1 cm^{-1} resolution and at room temperature. Mössbauer spectra of powder samples were collected in a standard transmission geometry using a radioactive source of ^{57}Co in Rh matrix (50 mCi) at room temperature. A calibration was done using a 25 µm thick natural foil; isomer shifts values are referred to α-iron. Magnetization measurements were performed by SQUID magnetometer (MPMS XL-5) in the temperature range from 2 to 750 K and in applied magnetic fields up to 5 T. Magnetic measurements were performed on $NdFeO_3$ nanoparticles and powdered $NdFe_{x-1}Mn_xO_3$ samples.

3. Results and discussion

The material particle size reduction down to nano- dimensions may result not only in remarkable changes of physical properties, like magnetic phase temperature, size dependence of saturation magnetization and coercive field but also in the emergence of the qualitatively new one, like superparamagnetism. Very similar situation can be observed in the case of proper substitution, for instance if the Fe^{3+} ion, which is inactive Jahn-Teller (JT) ion, is substituted by the Mn^{3+} JT active ion. In such a case the electronic properties and electron phonon-coupling can change significantly.

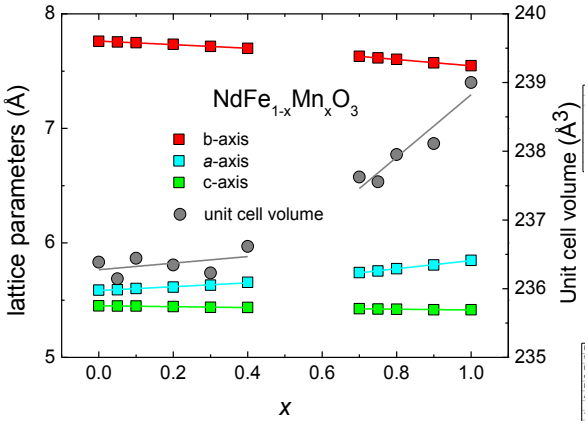

Figure 3. Evolution of lattice parameters and the unit cell volume with substitution.

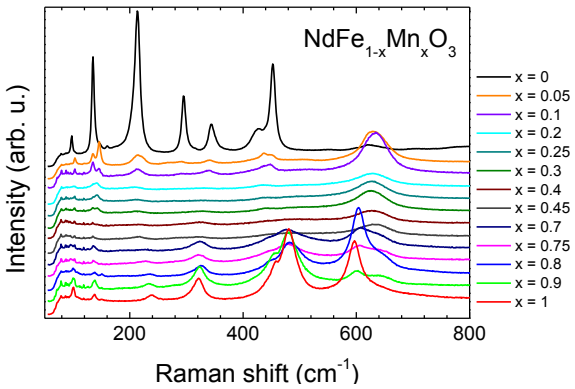

Figure 4. Unpolarised Raman spectra, recorded at room temperature for several compositions.

3.1. Crystal structure and Raman spectroscopy

The analysis of SEM images taken from $NdFeO_3$ NAPs (Figure 1.) revealed that aggregations of very well crystalized cuboid micro-sized particles with large distribution of size are randomly spread on the surface of agglomerates which are built from NAP with relatively uniform size. The amount of NAP agglomerates in the sample is higher than 90%. The average particle size, which was determined from SEM photos, increases from about 15 nm for as prepared NAP to about 25 nm for annealed NAP. In agreement with [5] both samples adopt orthorhombic crystal structure (space group *Pnma*). The relatively broad peaks in XRD pattern indicate presence of NAP in the sample (Figure 2).

No parasitic inclusions, secondary phases or concentration gradients were observed either by SEM methods including EDX analysis on $NdFe_{x-1}Mn_xO_3$ ingots or from XRD on powders. The substitution of the Mn^{3+} for the Fe^{3+} ion introduces both the JT distortions of the unit cell and distortion resulting from structural mismatch. The symmetry of the orthorhombic crystal structure (space group *Pnma*) remains unchanged in the whole concentration range. The lattice parameters and the unit cell volume change non-monotonically with substitution showing two distinguished regions below and above x = 0.5 (Figure 3). In the high Fe - concentration region with $x \leq$ 0.4 the unit cell volume is almost intact by substitution and lattice distortion is given mainly by tilting of Mn/FeO_6 octahedrons. The unit cell volume increases on further substitution and the lattice distortion can be attributed to both the JT distortion and the tilting of octahedrons.

Unpolarised Raman spectra of $NdFe_{x-1}Mn_xO_3$ which were recorded at room temperature are shown in Figure 4. The Raman spectra of the parent compounds $NdFeO_3$ and $NdMnO_3$ are in good agreement with published data, corroborating the orthorhombic symmetry space group *Pnma* of both compounds [6, 7]. Factor group analysis considering the site symmetry for the Γ-point phonons of orthorhombic $NdFeO_3$ indicates that the following 24 modes are Raman active among 60 zone-center phonon modes in the *Pnma* structure: $\Gamma_{Raman} = 7A_g+5B_{1g}+7B_{2g}+5B_{3g}$. As the Mn-content increases, the Raman bands become broader and the peak between 620 and 635 cm^{-1} dominates in the spectra up to x = 0.45. This peak can correspond to the peak at 643 cm^{-1} which was observed in room-temperature second-order Raman spectra of the orthorhombic $NdFeO_3$ single crystal [6] and was attributed to a two-phonon scattering caused either by two B_{1g} phonons or by two B_{2g} phonons. The observed mode was assigned as Fe-O breathing mode [6]. Features typical for the Raman spectrum of $NdMnO_3$ [7] become dominant for Mn concentration higher than x = 0.70. The Raman mode B_{2g} at 606 cm^{-1} is assigned to in-plane O_2 stretching leading to JT distortions. The change of the Raman profile along with the unit cell volume at x = 0.4 point toward the probable switch between JT non-distorted dominated regime to JT distorted dominated regime.

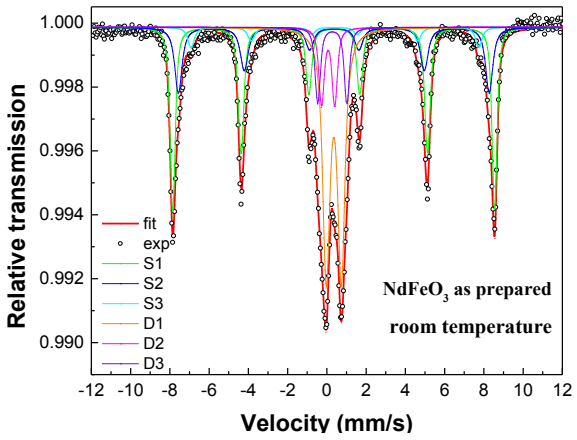

Figure 5. Mössbauer spectrum of as prepared $NdFeO_3$ nanoparticles.

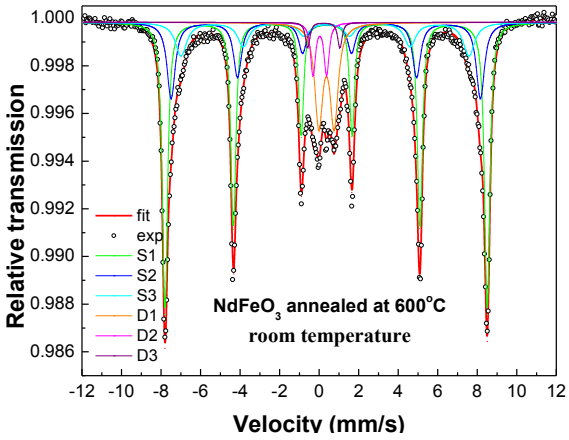

Figure 6. Mössbauer spectrum of $NdFeO_3$ nanoparticles annealed at 600°C/2h.

3.2. Mössbauer spectroscopy

The six fold coordinated Fe^{3+} ion of $NdFeO_3$ crystal is sitting in the centre of an octahedron and is in high spin state. The corresponding room temperature Mössbauer spectrum consists of a single sextet component [8]. Our results shows that the fit of the room temperature Mössbauer spectra for both as prepared and annealed $NdFeO_3$ nanoparticle samples is based on the superposition of three sextet and quadrupole doublet components (Figure 5 and Figure 6). The invariant values of hyperfine parameters δ and ε in all sextets confirm that the components describe the same iron crystal site (Table 1). Different values of hyperfine field B_{hf} in three sextet components indicate several slightly different local surroundings of the Fe^{3+} ions. The relative area of doublet components is reduced with the annealing of nanoparticle sample, i.e. with the increase of mean particle size (Table 1). Such an effect indicates that the observed doublet components can be attributed to the fraction of Fe^{3+}, which is in the superparamagnetic state at room temperature.

Table 1. ^{57}Fe Mössbauer parameters calculated from recorded spectra; *af*-area fraction of total, B_{hf}-hyperfine induction, δ-isomer shift, ε- quadrupole shift.

Sample	$NdFeO_3$ SHS as prepared				$NdFeO_3$ SHS 600°C/2h			
Sextet / Doublet	*af*	B_{hf} [T]	δ [mm/s]	ε [mm/s]	*af*	B_{hf} [T]	δ [mm/s]	ε [mm/s]
S1	0.275	50.5	0.37	–0.05	0.475	50.6	0.37	–0.03
S2	0.075	48.5	0.36	–0.06	0.207	48.6	0.37	–0.06
S3	0.171	46.0	0.37	–0.08	0.130	45.3	0.34	–0.08
S	0.521	48.7			0.812	49.3		
D1	0.292		0.36	0.79	0.130		0.37	0.78
D2	0.092		0.14	0.71	0.040		0.04	0.69
D3	0.095		0.28	1.40	0.017		0.23	1.63
D	0.479				0.188			

The room temperature Mössbauer spectra of $NdFe_{1-x}Mn_xO_3$ contain only sextets. The analysis of these spectra is summarized in Table 2. The width of peaks increases with increasing content of Mn. In the analysis of spectra we consider various environments around octahedral Fe^{3+} ions due to random distribution of Mn^{3+} ions. The probability of octahedral site having *n* nearest neighbor of Mn is:

$$P(n,\ x) = \frac{6!}{n!\,(6-n)!}(x)^n(1-x)^{6-n}$$

where *x* is concentration of Mn and *n* is the number of Mn ions among the nearest - neighbor Fe^{3+} ions.

Table 2. ^{57}Fe Mössbauer parameters calculated on the basis of recorded spectra; *af*-area fraction of total, *prob*-probability of surrounding, B_{hf}-hyperfine induction, δ-isomer shift, ε- quadrupole shift/splitting.

Sample	$NdFeO_3$				$NdFe_{0.8}Mn_{0.2}O_3$				
Sextet	*af*	B_{hf} [T]	δ [mm/s]	ε [mm/s]	*af*	*prob*	B_{hf} [T]	δ [mm/s]	ε [mm/s]
S1	1.0	51.39	0.369	-0.006	0.17	0.26	50.99	0.366	-0.147
S2					0.28	0.39	49.17	0.374	-0.006
S3					0.30	0.25	46.88	0.373	-0.012
S4					0.15	0.08	44.29	0.381	-0.016
S5					0.07	0.02	41.15	0.369	0.058
S6					0.03	<0.01	37.23	0.340	0.298
S		51.39					47.16		

3.3. Magnetic properties

The magnetic transition at T_{N1} and the spin-reorientation temperature T_{SR} were determined from magnetization measurements $\mu(T)$ (Figure 7). Spin reorientation is a more general phenomenon observed in many rare-earth orthoferrites. In the case of $NdFeO_3$ a spin reorientation transition is observed between 100 and 200K with gradual changes of the directions of the Fe^{3+}ordered magnetic moments [1]. In our paper we defined T_{SR} as the temperature at which the process of reorientation is finished and we assign it to the local minimum on $\mu(T)$ curve (Figure 7). The reduction of dimensionality to nano-scale decreases T_{SR} from 85 K to 20 K. Synthesis of NAP introduces distortion of lattice which can be considered as an effective barrier for spin reorientation and as result the reorientation process is finished at lower temperature. The substitution has an opposite effect and T_{SR} is rising with increasing content of Mn from 85 K to 123 K, 177 K, 223 K, 267 K and 283 K for x = 0.00, 0.10, 0.15, 0.20, 0.3 and 0.4, respectively. The magnetic moment of Mn^{3+} is smaller and energy required for spin reorientation is smaller too and therefore the T_{SR} increases with Mn concentration.

The Néel temperature T_{N1} was determined from a minimum on the $d\mu/dT(T)$ curve. System of NPA contains superparamagnetic particles and the magnetic interaction can be reduced due to surface effect that is why the magnetic transition occurs at lower temperature T_{N1} = 544 K. The magnetic transition of $NdFe_{1-x}Mn_xO_3$ becomes broader and T_{N1} decreases from 691 K to 356 K for x = 0.4 with Mn doping (Figure 8). Broadening of the transition can be attributed to enhanced probability of different surroundings of Fe with substitution as it was already considered in the analysis of Mössbauer spectra. The transition from paramagnetic to canted antiferromagnetic state is accompanied in several cases with sharp peak on $\mu(T)$ curves (Figure 8), which can be attributed to Hopkinson effect. Such a peak

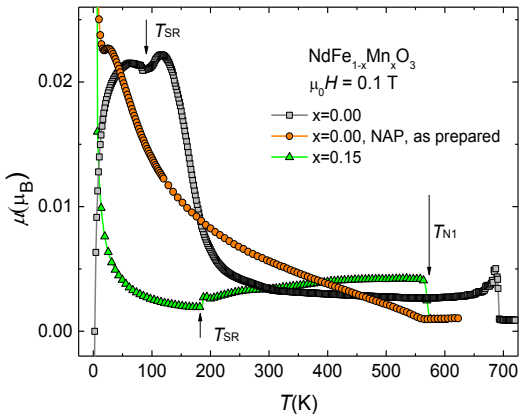

Figure 7. Effect of sample preparation on the reorientation and the magnetic phase transition.

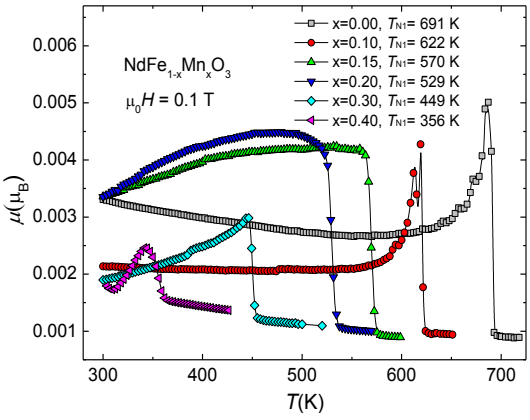

Figure 8. Effect of substitution on the magnetic phase transition at T_{N1}.

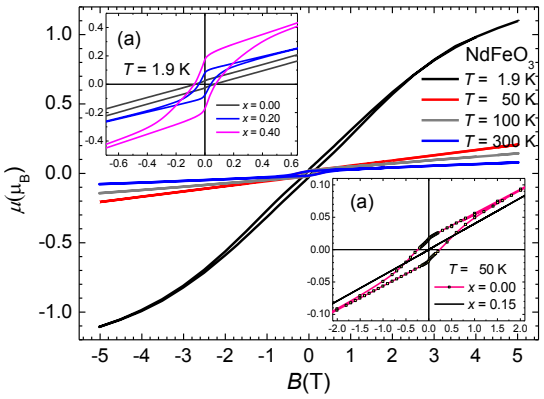

Figure 9. Effect of substitution on magnetic hysteresis loops.

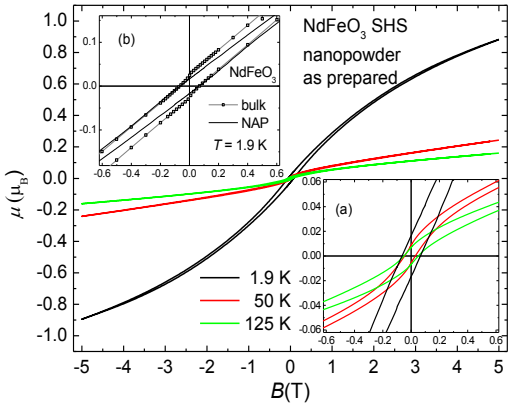

Figure 10. Effect of sample preparation – size dimension on magnetic hysteresis loops.

indicates that ferromagnetic component can be strong. The reduction of T_{N1} can be explained by weakening of magnetic interaction due to reduction of magnetic moment on average magnetic ion due to substitution with Mn^{3+} having smaller magnetic moment than Fe^{3+}.

Characteristic feature of $\mu(B)$ magnetization curves of $NdFeO_3$ is the presence of hysteresis loop in all temperature ranges (Figure 9 and Figure 9(a) and (b)). Loops appear at low magnetic field while linear dependence of $\mu(B)$ is observed in high fields above 50 K. The slope of linear part of $\mu(B)$ curves, corresponding to the high field susceptibility, increases with decreasing temperature down to 50 K which is consistent with antiferromagnetic magnetic ordering having a ferromagnetic component. The magnetic loop has S-shape at 1.9 K indicating the change of magnetic ordering in the vicinity of T_{N2}. Magnetizations taken at 1.9 K for 5 T show nearly no change for small concentrations of Mn and an increase at higher concentrations (μ_{5T} = 1.098 μ_B, 1.073 μ_B, 1.096 μ_B, 1.131 μ_B, 1.304 μ_B, 1.412 μ_B for x = 0.00, 0.10, 0.15, 0.20, 0.30 and 0.40, respectively). Remnant magnetization and coercive force increase with substitution (Figure 9(b)). Ferromagnetic component can be suppressed by Mn substitution in the range between T_{SR} and 5 K as it is indicated by absence of hysteresis loop in this region for x = 0.15 (Figure 9 (a)). The reduction of particle size to nano scale does not change $\mu(B)$ curves drastically (Figure 10). Main features of bulk material like presence of hysteresis loop (Figure 10(a)) are still present only the magnetization at 1.9 K is slightly reduced to 0.88 μ_B and tiny changes in the shape of the loop (Figure 10(b)) indicates that T_{N2} can be reduced, too.

Acknowledgment
This work was supported by projects VEGA 2/0178/13 and ERDF EU with No. ITMS26110230097.

References

[1] Sławiński W, Przeniosło R, Sosnowska I and Suard E 2005 *Journal of Physics* (Condens. Matter 17) 4605–4614
[2] Bartolomé J, Palacios E, Kuźmin M D and Bartolomé F 1997 *Physical Review* B **55** 11432
[3] Mrakovic A, Blanusa J, Primc D, Perovic M, Jaglicic Z., Kusigerski V, Spasojevic V 2013 *Ceramics International* **39**, 3771 , DOI: 10.1016/j.ceramint.2012.10.216.
[4] Mihalik M jr, Mihalik M, Fitta M, Bałanda M, Vavra M, Gabáni S, Zentková M, Briančin J 2013 JMMM, 345, 125–133
[5] Wang Y, Yan X, Chen J, Deng J, Yua R and Xing X 2014 *CrystEngComm*,16, 858-862
[6] Manoj K. Singh, Hyun M. Jang, H. C. Gupta and Ram S. Katiyar, J. Raman Spectrosc. 2008; 39: 842–848
[7] Iliev M N, Abrashev M V, Laverdière J, Jandl S, Gospodinov M M, Wang Y-Q and SunY-Y 2006 *Physical Review* B **73** 064302
[8] Eibschütz M, Shtrikman S and Treves D 1967 *Physical Review* **156** 562